Pergamon

Cement and Concrete Research, Vol. 25, No. 6, pp. 1179–1190, 1995

0008-8846/95 $9.50 + .00

0008-8846(95)00110-7

PROBABILITY OF CORROSION INDUCED CRACKING IN REINFORCED CONCRETE

Marita L. Allan
Energy Efficiency and Conservation Division
Department of Applied Science
Brookhaven National Laboratory
Upton, New York, 11973

(Refereed)
(Received March 4, 1994; in final form May 15, 1995)

ABSTRACT

A probabilistic approach to corrosion induced cracking in reinforced concrete was investigated. Hydraulic pressurization at the reinforcement/concrete interface was used to simulate corrosion of reinforcement and cause fracture. The failure pressure data was analysed statistically and found to have right hand skew. Correlation between failure pressure and visual observations of fracture surfaces suggested a possible change in failure mechanism depending on the presence of voids near the reinforcement. The failure pressure distributions were analysed to determine whether Weibull statistics could provide an adequate description. The effects of variables such as toughness, flaw size, corrosion products and corrosion rate on the shape of failure probability-time relationships were predicted.

Introduction

Reinforced concrete is at risk of loss of serviceability due to corrosion induced cracking. Design and construction of reinforced concrete infrastructure and nuclear waste disposal facilities requires consideration of the most effective means of optimizing service life. Quantitative prediction of the cracking of concrete due to corrosion of reinforcement and of the factors that control the resistance to cracking is necessary to achieve maximum performance. Mathematical models have been used to estimate the time to corrosion induced cracking (1,2). Field or laboratory data can be combined with modelling to produce empirical equations for prediction of the time to cracking (3) or to estimate the time to necessary rehabilitation (4).

The time to corrosion initiation is usually modelled as transport of aggressive species, such as chlorides, or of a carbonation front to the depth of reinforcement (1,2,5,6). The typical approach to failure prediction once corrosion is initiated is to estimate the rate of corrosion and calculate the time to failure based on development of a critical stress to cause concrete cracking

(1). The induced stress is calculated from the expansion of the reinforcement due to corrosion. Finite element modelling has been used to estimate the amount of corrosion necessary for failure (7,8).

Corrosion induced cracking of concrete involves two major stages. Firstly, a layer of corrosion products forms at the interface between the reinforcement and the cover concrete. The corrosion layer effectively causes disbondment between original steel and concrete. Proceeding the disbondment stage is the formation of through-thickness cracks or spalls in the concrete surrounding the corroded reinforcement. The term "failure" is used in this paper to describe the combination of disbondment and through-thickness concrete cracking. The stress at which corrosion induced cracking or spalling occurs depends on the critical flaw sizes at the reinforcement/concrete interface and in the concrete surrounding the anodic area of the reinforcement. Fracture based failure criteria are appropriate for prediction of disbondment at the reinforcement/concrete interface and cracking of the cover concrete. It is feasible to incorporate a fracture mechanics criterion in prediction of corrosion-induced cracking (7).

Deterministic models of failure do not allow for any random error in predicting a response, such as time to cracking, to a variable, such as depth of cover. Concrete is inherently heterogenous and it is unrealistic to predict a single value of time to failure for a given set of variables. Mechanical, fracture and physical properties of concrete vary on both the micro- and macro-scales. Thus, deterministic models cannot provide an adequate representation of concrete cracking. The weaknesses of deterministic models can be overcome by using probabilistic models to describe failure. Probabilistic models are used extensively to predict reliability of equipment, components, materials and systems (9-12). It follows that corrosion induced cracking in concrete can be described by a continuous distribution function and that such a description should enhance the accuracy and realism of failure prediction.

Probability methods for predicting the life of concrete were discussed by Clifton (13) who noted that lack of data to determine statistical parameters is inhibiting the application of such methods. This paper reports the fitting of failure probability distributions to failure data for reinforced concrete obtained from experimental simulation of reinforcement corrosion.

Experimental

Localized expansion of reinforcement embedded in concrete due to corrosion was simulated and used to cause disbondment and concrete cracking. The experimental method has been described previously (14). The technique involved localized hydraulic pressurization at the reinforcement/concrete interface to cause disbondment and cracking of cover concrete in a manner similar to that induced by corrosion. Hydraulic fracturing is frequently used in the field of geotechnology for testing rocks. Deformed reinforcement bars 12 mm in diameter were embedded axially in cylinders of concrete 50 mm in diameter. The bars were pre-drilled internally so that hydraulic oil could be pumped out of the bar and to the interface to cause pressurization. The expansion occurred in a localized region in order to simulate the early stages of localized corrosion. Simulation of corrosion to cause disbondment and concrete cracking is shown schematically in Figure 1.

The reinforced concrete specimens were cured for 28 days in a fog room prior to testing. A hydraulic cylinder was connected between the embedded reinforcement bar and a compression testing machine and used to deliver oil to the reinforcement/concrete interface at a constant rate.

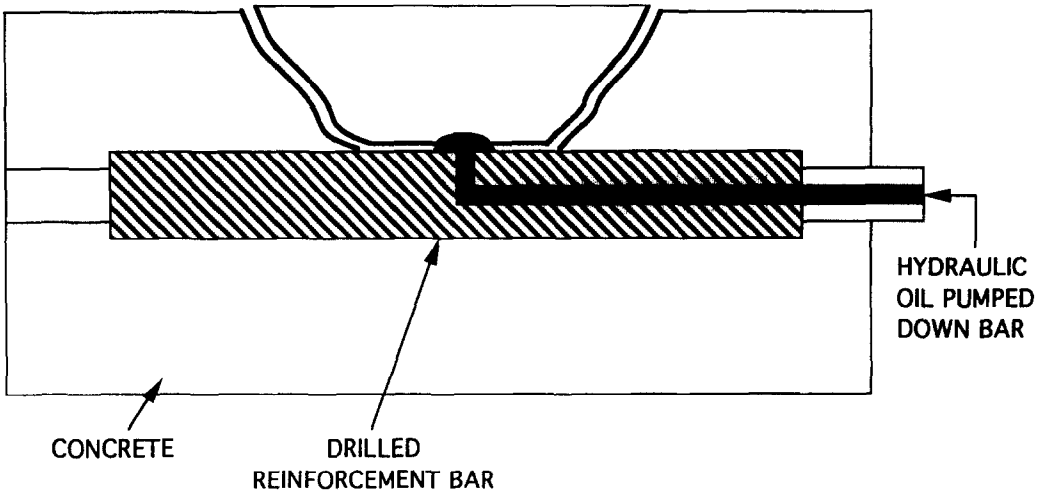

FIG. 1
Schematic Diagram of Specimen used for Hydraulic Pressurization.

Pressure versus time was monitored using a transducer. Failure corresponded to the maximum pressure and this occurred simultaneous to the appearance of concrete surface cracks. Examination of specimens revealed disbondment and concrete failure in a mode identical to that observed in practice.

In previously reported hydraulic pressurization studies, polymer tubing embedded in concrete was inflated uniformly using hydraulic oil and the pressure to cause cracking was measured (3, 15). Such studies assume uniform corrosion and do not consider the role of the reinforcement/concrete bond in the overall view of failure. The experimental arrangement used in the work reported in this paper includes the contribution of the reinforcement/concrete bond and the effect of non-uniform corrosion. Most models of corrosion consider expansion of reinforcement to be uniform. The approach used in this work is that corrosion will be localized

TABLE 1. Summary of Failure Pressure Results

Failure Pressure Results	Mix 1	Mix 2
Minimum Failure Pressure (MPa)	12.2	14.5
Maximum Failure Pressure (MPa)	68.3	54.3
Mean (MPa)	30.7	26.4
Standard Deviation (MPa)	15.3	9.0
Third Moment (MPa^3)	3.48×10^3	1.08×10^3
Fourth Moment (MPa^4)	1.58×10^5	3.17×10^4
Skewness Coefficient, β_1	0.95	2.88
Kurtosis Coefficient, β_2	1.48	4.82

in the initial stages, particularly if chloride ions are responsible, and that uniform corrosion is not a requirement for concrete cracking. If desired, the reinforcement bars could be drilled to simulate different expansion behaviour from that used in this study.

The effect of concrete mix proportions on failure pressure distribution has been reported (14). This paper examines the failure statistics of two of the concrete mixes studied. Three batches of 20 specimens were cast. A total of 59 specimens were tested for Mix 1 and 57 for Mix 2. The proportions for Mix 1 were 316 kg/m^3 ordinary Portland cement (Australian Standard 1315 Type A), 860 kg/m^3 washed river sand passing through a 1.18 mm sieve, 945 kg/m^3 9.5 mm crushed and washed basalt and 221 kg/m^3 water. The proportions for Mix 2 were 308 kg/m^3 cement, 983 kg/m^3 sand, 1032 kg/m^3 coarse aggregate and 232 kg/m^3 water. The materials were the same for both mixes. The 28 day compressive strengths were 29 ± 1 MPa and 25 ± 1 MPa for Mixes 1 and 2, respectively.

Results

Failure Pressures

The failure pressure data is summarized in Table 1. The third and fourth moments of the failure pressure distributions were calculated, along with the skewness and kurtosis coefficients, β_1 and β_2. The procedures for calculating the moments and coefficients are given in statistics texts (e.g. 9,12). The third moment of a distribution indicates skewness, with positive values associated with right hand skew, and negative values associated with left hand skew (16). The fourth moment indicates kurtosis, or peakedness of a distribution (16). A low value of the fourth moment indicates relatively few extreme items in a population while a high value indicates a greater proportion of extremes (9).

Histograms of the results were constructed and indicated that the data distributions were asymmetric. The third moments of the failure pressure distributions were calculated to be positive, therefore confirming right hand skew. The normal (Gaussian) distribution was found to be inadequate for describing the data due to the skewness. The fourth moments were high due to the significant number of outliers. There was no justifiable reason for rejecting the outliers.

Discussion

The significant variation in failure pressures for nominally identical specimens was attributed to the inherent variability in flaw sizes, concrete toughness and reinforcement/concrete bond toughness. The failure pressures showed a higher degree of scatter than the compressive strengths. This is due to the greater role of pre-existing flaws in failure for tensile-type loading. Post-failure examination of fracture surfaces by visual and optical microscope methods showed that failure pressures below approximately 22 MPa were typically associated with air voids at the reinforcement surface or in the surrounding concrete. This shows the significant contribution of flaws in controlling resistance to failure and demonstrates the necessity to use a fracture mechanics approach to failure description so that the influence of flaw size is included. Post-failure examination of specimens with higher failure pressures did not exhibit any obvious features to explain variability. It is hypothesized that the scatter in failure pressures above approximately 22 MPa is due to variation in the size of pre-existing microcracks which extend on pressurization.

The variability in the failure pressure data confirms the need to use a probabilistic

approach to failure prediction. A deterministic model of failure would predict a single value of failure pressure for each concrete mix since the mix proportions, depth of cover, curing conditions and age were constant. Such a model is inadequate. Variability in the pressure necessary to cause failure can be expected to be greater for real structures than for laboratory prepared specimens. Therefore, predicting the probability that failure of an element will occur after a certain amount of corrosion or time is more justified than predicting a lifetime which does not take into account the inevitable variability in concrete or microclimate.

Adequate description of the probability of failure requires choice of a suitable probability distribution. Distributions that are commonly used in statistical failure models include log normal, gamma and Weibull (9-11). A distribution should explain the data and have a physical basis for being appropriate (10). In other words, the distribution should be compatibility with the mechanism of failure. When fitting a distribution to observed data it must not be neglected that the number of samples may be inadequate for accurate description, especially if insufficient data exists to fully represent the tails of the distributions. Since failure prediction is usually more concerned with "worst-case" probability of failure, such as minimum service life, it is necessary that the chosen distribution function provide adequate fit especially in the lower tail.

The skewness of the failure pressure data suggests that a skewed distribution may provide an adequate fit. Selection of a suitable distribution can be narrowed by consideration of the skewness and kurtosis coefficients (9,12). These coefficients can be plotted against each other and used to distinguish between different distributions. Thus, sample estimates of β_1 and β_2 from the data can be compared with the points or lines describing different distributions and used to select a suitable distribution to represent the data. This procedure depends on the accuracy of the sample estimates of β_1 and β_2 in approximating the true values for the population. Extreme values, or outliers, will affect the values of the third and fourth moments used to estimate the skewness and kurtosis coefficients.

The sample estimates of β_1 and β_2 for Mix 1 fell below the line describing the Weibull distribution, whereas the estimated coefficients were close to the Weibull distribution line for Mix 2. The narrower distribution of failure pressures, and the absence of as many outliers for Mix 2 as compared with Mix 1, results in the fourth moment being less influenced by a few extreme values.

The Weibull distribution function (17) has been applied to failure statistics of brittle materials and it is therefore plausible that the distribution may describe the failure pressure data. The failure concept used by Weibull (17) is that of the weakest link of a chain, implying that failure of an object occurs when one of its parts fails. This theory can be extended to brittle materials since the entire brittle component fails when the stress intensity at one flaw within the component reaches the critical value required for crack propagation (11,18). The Weibull function has been applied to tensile bond strength between rock and cement paste by Monteiro and Andrade (19) and has been discussed in relation to concrete by Clifton (13), Bazant et al. (20,21) and Carpinteri (22).

The Weibull distribution can be used in two different forms for the description of failure (11,18). The three-parameter distribution includes a term for the minimum stress below which failure is not expected. This is termed the "threshold strength" or "location parameter". The two-parameter Weibull distribution sets the threshold stress to zero. Selection of this lower bound depends on the system studied. The threshold stress is usually estimated as zero or as a value

slightly below the lowest observed failure stress. For corrosion of steel in concrete it is plausible that a finite amount of corrosion products, and therefore induced pressure, can be accommodated before the probability of failure exceeds zero. This is particularly so if concrete is viewed as being quasi-brittle and if air voids and pre-existing microcracks can be filled with corrosion products. The pressure-time curves recorded during hydraulic pressurization and the failure pressure data indicated that some critical value was required before catastrophic cracking occurred. Thus, use of a three-parameter distribution appears warranted. This would also be the case in real life failure prediction since a critical period of corrosion propagation would be required before failure is probable.

Weibull plots were constructed by plotting lnln [1/(1 - Failure Probability)] against ln (Failure Pressure - Threshold Pressure). The threshold pressure was varied and the sample correlation coefficient was calculated. The two-parameter and three-parameter Weibull plots are shown in Figures 2 and 3. The threshold pressure giving the most linear fit is shown.

A linear plot would be expected if the Weibull distribution describes the data adequately. The distribution exhibited the poorest fit in the right hand tail. In addition to appraisal of the linearity of the Weibull plots, the observed and expected numbers for given categories of failure

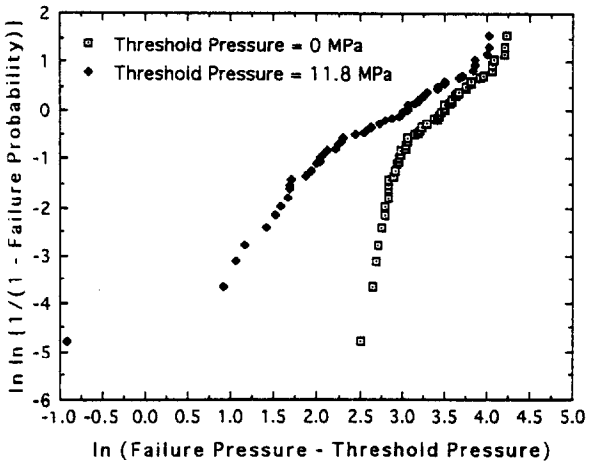

FIG. 2
Weibull Probability Plot for Mix 1.

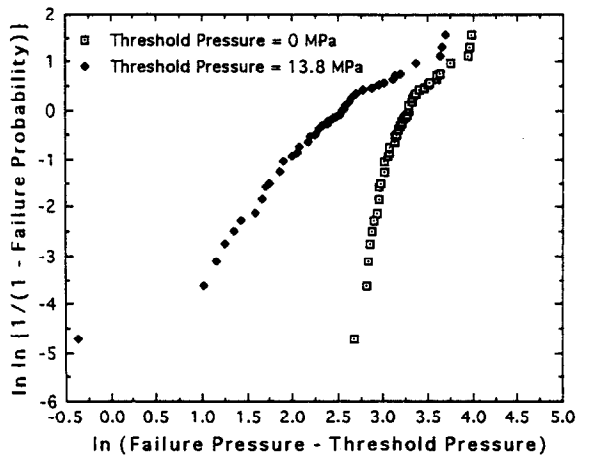

FIG. 3
Weibull Probability Plot for Mix 2.

pressure were compared and chi-square (χ^2) goodness of fit tests were conducted. Categories of pressure were selected and combined if necessary to give an expected value of at least 5 in each category (12). This procedure tends to reduce the effect of outliers and this fact should not be neglected. Following the chi-square tests, the hypothesis that the data from Mix 1 could be described by a three-parameter Weibull function was rejected at the 5% significance level, but was accepted for Mix 2. The hypothesis that the data followed a two-parameter Weibull function was rejected for both mixes.

The possibility that the pressure to cause cracking and spalling follows a bimodal distribution should not be dismissed. There is a physical justification for this based on the visual observations of failed specimens. Low failure pressures were typically associated with the presence of air voids in the stressed zone. The cumulative failure probability distributions for all three tested mixes were almost identical below approximately 22 MPa (14). It is proposed that the similarity in failure pressure distributions in the low pressure region is due to the similarity in size distribution and size variance of air voids. Above 22 MPa the shape of the distributions is believed to reflect the variability in the size of pre-existing microcracks. It is plausible that two different failure mechanisms exist, depending on the presence of air voids and

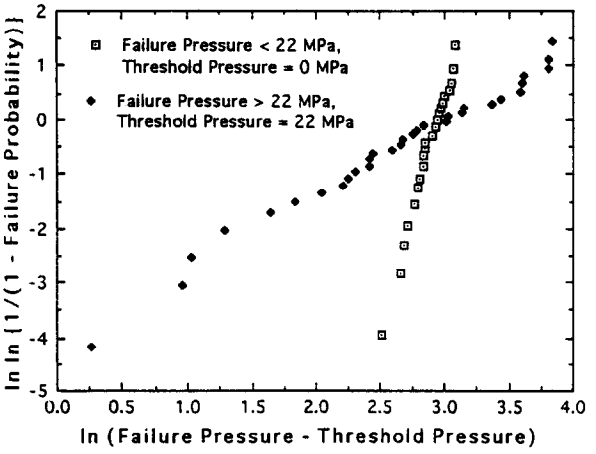

FIG. 4
Weibull Probability Plot for Mix 1 Subsets.

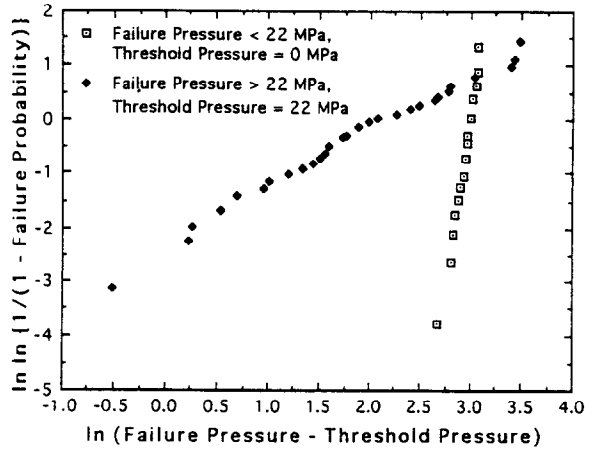

FIG. 5
Weibull Probability Plot for Mix 2 Subsets.

that this may result in a bimodal or mixed failure probability distribution. The Weibull plots exhibited a possible change in slope around 22 MPa.

The data was split into two subsets for each mix, below and above 22 MPa, and analysed for compatibility with a Weibull description. The resultant Weibull plots are depicted in Figures 4 and 5. The plots show improved linearity compared with the complete data sets. Inclusion of a threshold pressure for the data subset below 22 MPa did not improve linearity. Chi-square goodness of fit tests were conducted and the hypothesis that the results follow a Weibull distribution was not rejected at the 5% significance level. The steeper slope of the plot for data <22 MPa indicates a higher Weibull modulus and a lower degree of data scatter.

It would be erroneous at this stage to overreach the above findings from the experimental data and conclude that the Weibull distribution is unequivocally appropriate or inappropriate for description of failure of concrete structures due to corrosion of reinforcement, or that a bimodal distribution is necessarily correct. A larger data set would improve the confidence of fitting a distribution to the experimental data, particularly in the upper and lower tails. Chi-square goodness of fit tests would also be more reliable with more data. Considering field data with experimental data is also desirable in selection of a distribution to predict failure of real life structures.

The validity of applying classical Weibull statistics to reinforced concrete has been questioned, with particular reference to size effect (20,21). Shortcomings of classical Weibull theory with respect to reinforced concrete include disregard of stress redistribution and energy release that occur during stable macrocrack growth that precedes failure and treatment of a structure as a uniaxial bar with variable cross-section (20). Modifications to the application of Weibull statistics have been proposed (21).

Factors Controlling Failure Probability Distribution

Figure 6 gives a schematic view of the relationship between failure probability and pressure. The figure is based on the results obtained from the hydraulic pressurization tests. Pressure induction is required before the probability of failure exceeds zero at pressure P_i. Failure probability equals 1.0 when pressure reaches $P_{1.0}$. The form of a failure probability-pressure curve will change with different geometries and concrete properties. Factors such as reinforcement/concrete bond toughness, cover concrete toughness and depth of cover are predicted to increase the pressure required for disbondment and concrete cracking. The size of flaws at the reinforcement/concrete interface and in the concrete surrounding the anode will also influence failure pressure. The failure pressure will decrease with increasing size of anode and concrete voids and microcracks.

The shape of a failure probability-time curve will depend on the time to corrosion initiation, the rate of pressure development and the type of corrosion products, in addition to the factors that control failure pressure. A schematic diagram of failure probability versus time is shown in Figure 7. The time to corrosion initiation is termed t_i. Following initiation is a period of corrosion activity in which pressure starts to develop. This is termed the "pressure induction period". Once a critical pressure is reached the probability of failure exceeds zero at time t_f. Failure probability exceeds zero after a period of corrosion activity, rather than the time at which corrosion commences. Ultimately, the probability of failure equals 1.0 at time $t_{1.0}$.

For concrete with air voids surrounding the anode there will be an extended period of corrosion before pressure develops at the reinforcement/concrete interface. This effect was observed in the pressure-time curves obtained for the hydraulic pressurization tests when large air voids were located at the interface. Large air voids have also been observed to act as repositories for corrosion products and to increase the time to failure (23-25). In contrast, concrete with low porosity and few pre-existing microcracks contains little space for accumulation of voluminous corrosion products and these products are therefore confined and exert pressure on surrounding concrete. A schematic representation of the role of voids located near the corroding reinforcement is presented in Figure 8 and is based on failure observations from accelerated corrosion tests and field studies. Elastic modulus of the cover concrete may also be influential in controlling the amount of corrosion that can accumulate at the interface before failure.

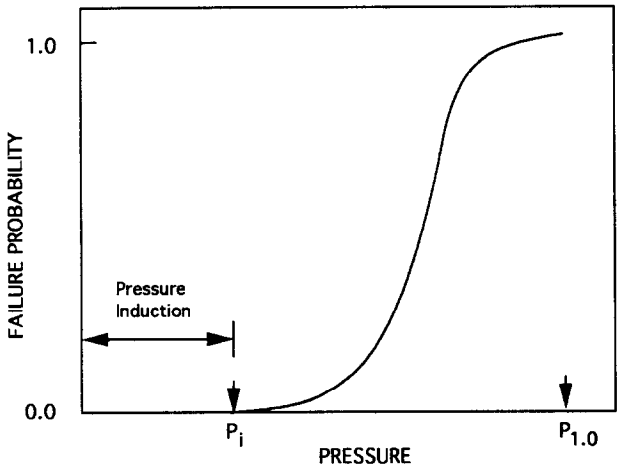

FIG. 6
Schematic Failure Probability-Pressure Curve.

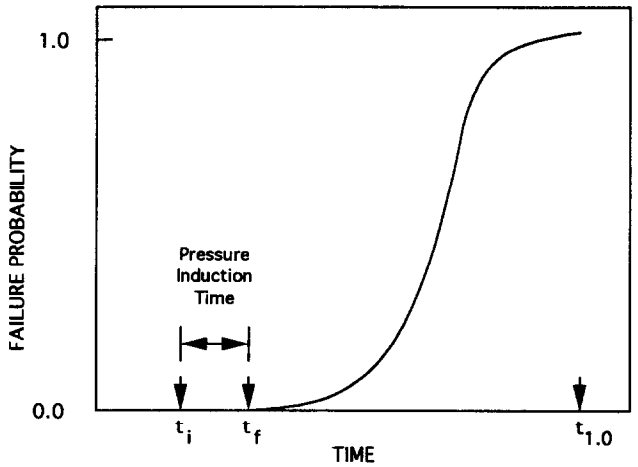

FIG. 7
Schematic Failure Probability-Time Curve.

The pressure induction time for porous concrete is expected to be greater than that for dense concrete with few voids located at or near the reinforcement. If a concrete contains a substantial degree of interconnected pores, voids and microcracks then the corrosion initiation time, t_i, will be decreased if corrosion is due to penetration by aggressive species. Thus, the competing effects of corrosion initiation time and pressure induction time will ultimately determine the time at which failure probability exceeds zero in very porous, permeable concrete. This does not imply that a porous, permeable concrete is desirable since the overall loss of reinforcement is predicted to be greater as a result of prolonged corrosion activity prior to development of significant pressure. Once pressure does develop the failure of porous concrete is predicted to occur at a relatively low pressure due to the reduced stress required for crack propagation.

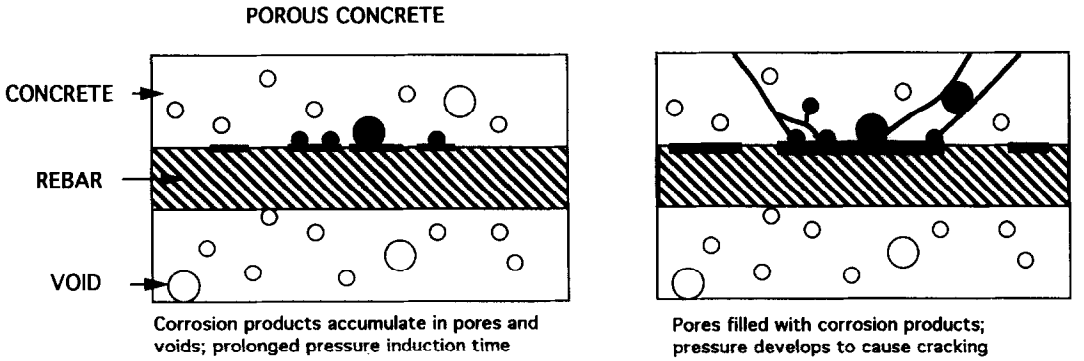

FIG. 8
Progress of Corrosion in Porous Concrete.

The period of pressure induction should be reduced at higher corrosion rates. Therefore, the time between initiation at t_i and failure probability exceeding zero at t_f should be shortened. The form of the failure probability-time curve will also depend on the type of corrosion product formed since iron oxides and hydroxides have different molar volumes. For example, Fe_3O_4 has a lower molar volume than $Fe_2O_3.2H_2O$. In oxygen deficient conditions where production of Fe_3O_4 is favoured, the rate of pressure development and, hence, time to achieve critical pressures should be greater than when $Fe_2O_3.2H_2O$ is produced due to the reduced rate of expansion even when corrosion rates are equal. The predicted effects of corrosion rate and corrosion products on the failure probability-time curve are shown in Figure 9.

Increasing the toughness of concrete and the bond between reinforcement and concrete should effectively increase the pressure induction time (if all other variables are held constant) and increase the pressure required for failure. The predicted effect should be similar to that depicted in Figure 9. Decreasing the variability of concrete, particularly the variability of toughness and flaw sizes (i.e. pre-existing microcracks, pores and voids) should decrease the time lapse between failure probability exceeding zero at t_f and failure probability equalling 1.0 at $t_{1.0}$. Reducing concrete variability is a primary means of reducing variability in risk of failure.

Applications of Hydraulic Pressurization and Statistical Techniques

Hydraulic pressurization can be used to determine quantitatively the factors that control

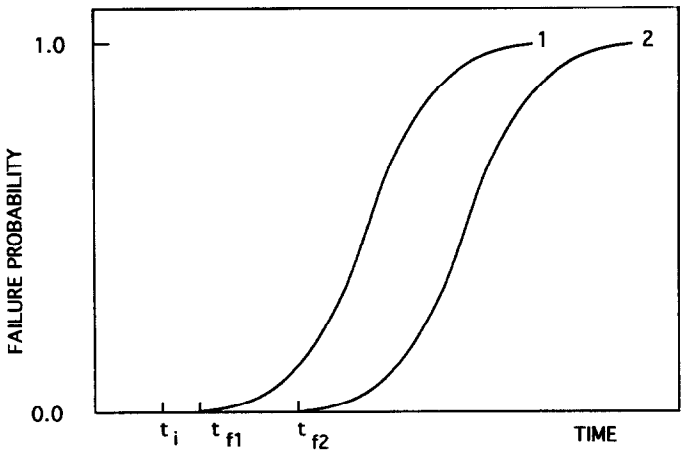

FIG. 9
Predicted Effects of Corrosion Rate and Corrosion Products on Failure Probability-Time Curve (All other variables assumed constant).

failure pressure and failure probability. The technique provides actual data rather than values predicted from empirical models and is also valuable for elucidation of failure mechanisms. Means of optimizing the service life and reducing performance variability though design can be identified and quantified through such experiments. For example, tests could be used to establish the effects of different geometries, mix designs, reinforcement surfaces or depths of cover. This would be particularly useful in assessing the failure resistance and failure sensitivity of new mix designs and materials for which an extensive track record is unavailable. Determination of the role of toughening mechanisms such as addition of fibres is also possible.

It is desirable to calibrate the experimentally measured failure pressures and derived probabilities against case histories to provide a more global view of life prediction. From this, greater understanding of failure predictive methods and the applications of statistics could be achieved. Prediction of failure pressure distribution needs to be combined with predictive methods for corrosion initiation time and corrosion rate.

Conclusions

Corrosion induced cracking of concrete can be simulated by hydraulic pressurization at the reinforcement/concrete interface. The hydraulic pressurization technique can be used to determine the quantitative effects of variables on the pressure required for cracking and spalling of concrete. Failure pressures for a given concrete mix and geometry were found to be highly variable due to the inherent variability in controlling factors such as toughness and size and type of flaws. Thus, a probabilistic approach to failure was studied. A Weibull distribution function appeared adequate to describe the failure pressure distribution of one tested mix, but not the other. The possibility that failure pressure may follow a bimodal distribution due to changes in failure mechanisms associated with the presence of voids was investigated. Initial analysis suggests that a bimodal distribution may be plausible. Before arriving at a definitive conclusion

as to which distribution is most appropriate, it is necessary to analyse more experimental data and combine this with field data in order to confirm the validity of statistical models and relate them to practice.

Acknowledgements

The experimental work reported in this paper was conducted while the author was a postgraduate student in the Department of Materials Engineering, Monash University, Australia. The work was supervised by B.W. Cherry and supported by a Monash Graduate Scholarship. Thanks to C.C. Berndt, SUNY at Stony Brook, for assistance with the statistical analysis.

References

1. Bazant, Z.P., J. Struct. Eng., ASCE, 105 (ST6), 1137 (1979).
2. Tuutti, K., CBI Forskning Research Fo, 4.82, Stockholm (1982).
3. Morinaga, S., Proceedings of 2nd Australia-Japan Workshop on Durability of Reinforced Concrete, Melbourne (1988).
4. Cady, P.D. and Weyers, R.E., J. Trans. Eng., 110, 34 (1984).
5. Clifton, J.R. and Pommersheim, J.M., NISTIR 4954, National Institute of Standards and Technology (1992).
6. Walton, J.C., Plansky, L.E. and Smith, R.W., NUREG/CR-5542, US Nuclear Regulatory Commission (1990).
7. Dagher, H.J. and Kulendran, S., ACI Struct. J., 89, 699 (1993).
8. Molina, F.J., Alonso, C. and Andrade, C., Mat. and Struct., 26, 532 (1993).
9. McCormick, N.J., Reliability and Risk Analysis, Academic Press, New York (1981).
10. Mann, N.R., Schafer, R.E. and Singpurwalla, N.D., Methods for Statistical Analysis of Reliability and Life Data, John Wiley and Sons, New York (1974).
11. Bury, K.V., Statistical Models in Applied Science, John Wiley and Sons, New York (1975).
12. Hahn, G.J. and Shapiro, S.S., Statistical Models in Engineering, John Wiley and Sons, New York (1967).
13. Clifton, J.R., ACI Mat. J., 90, 611 (1993).
14. Allan, M.L. and Cherry, B.W., Corrosion, 48, 426 (1992).
15. McLeish, A., Technical Note 1632, Taywood Engineering, Southall (1986).
16. Pazer, H.L. and Swanson, L.A., Modern Methods for Statistical Analysis, Intext, New York (1972)
17. Weibull, W., J. of App. Mech., 18, 293 (1951).
18. Davies, D.G.S., Proc. Brit. Ceram. Soc., 22, 429 (1973).
19. Monteiro, P.J.M. and Andrade, W.P., Cem. and Conc. Res., 17, 919 (1987).
20. Bazant, Z.P., Xi, Y. and Reid, S.G., J. Eng. Mech., ASCE, 117, 2609 (1991).
21. Bazant, Z.P. and Xi, Y., J. Eng. Mech., ASCE, 117, 2623 (1991).
22. Carpinteri, A., Mechanical Damage and Crack Growth in Concrete, Martinus Nijoff, Dordecht (1986).
23. Allan, M.L. and Cherry, B.W., Corrosion Australasia, 16, (3/4), 15 (1991).
24. Tuutti, K., in Malhotra, V.M. ed., Performance of Concrete in Marine Environment, ACI SP-65, Detroit, 223 (1980).
25. Treadaway, K.W.J., Cox, R.N. and Brown, B.L., Proc. Instn. Civ. Engrs., Part 1, 86, 305 (1989).